PROCEEDINGS OF SCIENCE

Measurement of $\eta_c(1S)$, $\eta_c(2S)$ and non-resonant $\eta'\pi^+\pi^-$ production via two-photon collisions

Qingnian Xu[*] [†]
Institute of High Energy Physics, Chinese Academy of Siceces
University of Chinese Academy of Sciences
E-mail: qingnian.xu@cern.ch

We report the measurements of $\gamma\gamma \to \eta_c(1S), \eta_c(2S) \to \eta'\pi^+\pi^-$ with η' decays to $\gamma\rho$ and $\eta\pi^+\pi^-$ using 941 fb^{-1} of data collected with the Belle detector at the KEKB asymmetric-energy e^+e^- collider. First observation of $\eta_c(2S) \to \eta'\pi^+\pi^-$ with a significance 5.5σ including systematic error is obtained. The products of the two-photon decay width and branching fraction of decays to $\eta'\pi^+\pi^-$ are determined for the $\eta_c(1S)$ and $\eta_c(2S)$, respectively. A new decay mode for the $\eta_c(1S) \to \eta' f_0(2080)$ with $f_0(2080) \to \pi^+\pi^-$ is observed with a statistical significance of 20σ. The cross section for $\gamma\gamma \to \eta'\pi^+\pi^-$ and $\eta' f_2(1270))$ are measured for the first time.

XXVI International Workshop on Deep-Inelastic Scattering and Related Subjects (DIS2018)
16-20 April 2018
Kobe, Japan

[*] Speaker.
[†] On behalf of the Belle Collaboration.

PoS(DIS2018)225

1. Introduction

The charmonium states $\eta_c(1S)$ and $\eta_c(2S)$ play important role in tests of quantum chromodynamics (QCD) [1]. Precise measurement of their two-photon decay widths may provide sensitive tests for QCD models [2]. The lowest heavy-quarkonium state $\eta_c(1S)$, together with the J/ψ, $\eta_b(1S)$, and $\Upsilon(1S)$, serve as benchmarks for the fine tuning of input parameters for QCD calculations [3]. The $\eta_c(1S)$ and $\eta_c(2S)$ resonance parameters were measured in $\psi(2S)$ radiative decay by BESIII, and in B decay and two-photon production by BaBar, Belle and CLEO [4, 5]. CLEO made the first measurement of the $\eta_c(2S)$ two-photon decay width $\Gamma_{\gamma\gamma}$ via $K^0_S K^+\pi^-$ but observed no signal for the $\eta_c(2S) \to \eta'\pi^+\pi^-$ decay [5].

The cross sections for two-photon production of meson pairs have been calculated in perturbative QCD and measured in experiments in a W region near or above 3 GeV, where W is the invariant mass of the two-photon system. The leading term in the QCD calculation [6] of the cross section predicts a $1/(W^6\sin^4\theta)$ dependence for a charged-meson pair. Here, θ is the scattering angle of a final-state particle in the two-photon CM frame. The handbag model [7] gives the transition amplitude describing energy dependence and predicts a $1/\sin^4\theta$ angular distribution for both charged- and neutral-meson pairs for large W. The Belle results for the cross sections [8] show that the angular distributions for the charged-meson pairs, $\gamma\gamma \to \pi^+\pi^-, K^+K^-$, agree well with the $1/\sin^4\theta$ expectation, while those for the neutral-meson pairs, $\gamma\gamma \to \pi^0\pi^0, K^0_S K^0_S, \eta\pi^0$ and $\eta\eta$, exhibit more complicated angular behavior. There is no specific QCD prediction for the two-photon production of either the pseudoscalar-tensor meson pair $\eta' f_2(1270)$ or the three-body final state $\eta'\pi^+\pi^-$. Our results for the production of these two- and three-body final states would thus provide new information to validate QCD models.

2. Belle detector and data sample

The Belle detector [9] consists of a silicon vertex detector, a 50-layer central drift chamber, an array of aerogel threshold Cherenkov counters, a barrel-like arrangement of time-of-flight scintillation counters, and an electromagnetic calorimeter (ECL) comprised of CsI(Tl) crystals located inside a superconducting solenoid coil that provides a 1.5 T magnetic field. An iron flux-return located outside of the coil to detect K^0_L mesons and to identify muons.

We use two data samples. The first is collected at the $\Upsilon(4S)$ resonance ($\sqrt{s} = 10.58$ GeV) and 60 MeV below it with integrated luminosity $L_{\rm int,4S}$ = 792 fb^{-1}, while the other is recorded near the $\Upsilon(5S)$ resonance ($\sqrt{s} = 10.88$ GeV) with $L_{\rm int,5S}$ = 149 fb^{-1}.

3. Event selection

At least one neutral cluster and exactly four charged tracks with zero net charge are required in each event. The candidate photons are neutral clusters in the ECL that have an energy deposit greater than 100 MeV. To suppress background photons from π^0 (π^0 or η) decays for the $\eta\pi\pi$ ($\gamma\rho$) mode, any photon that, in combination with another photon in the event has an invariant mass within the π^0 (π^0 or η) window $|M_{\gamma\gamma} - m_{\pi^0}| < 0.018$ GeV/c^2 ($|M_{\gamma\gamma} - m_{\pi^0}| < 0.020$ GeV/c^2 or $|M_{\gamma\gamma} - m_{\eta}| < 0.024$ GeV/c^2) is excluded. Events with an identified kaon ($K^\pm$ or $K^0_S \to \pi^+\pi^-$) or

proton are vetoed. The transverse momentum $|\Sigma p_t^*|$ tend to carry small transverse momentum. A $|\Sigma p_t^*|$ requirement allows significant background reduction. The $|\Sigma p_t^*|$ is optimized to be $|\Sigma p_t^*| < 0.15$ GeV/c for the $\eta\pi\pi$ mode and $|\Sigma p_t^*| < 0.03$ GeV/c for the $\gamma\rho$ mode. To improve the momentum resolution of the η', two separate fits to the η' are applied, one with a constrained vertex and the other with a constrained mass.

For both the $\eta\pi\pi$ and $\gamma\rho$ modes, we reconstruct $\eta'\pi^+\pi^-$ candidates by combining the η' with the remaining $\pi^+\pi^-$ pair, which must satisfy a vertex-constrained fit. The sum of the ECL cluster energies in the laboratory system and the scalar sum of the absolute momenta for all charged and neutral tracks in the laboratory system for the $\eta'\pi^+\pi^-$ system must satisfy $E_{\rm sum} < 4.5$ GeV and $P_{\rm sum} < 5.5$ GeV/c.

4. Measurtment of $\eta_c(1S)$ and $\eta_c(2S)$

The background in the $\eta'\pi^+\pi^-$ mass spectrum for the R measurement is dominated by three components: (1) non-resonant (NR) events produced via two-photon collisions, which have the same $|\Sigma p_t^*|$ distribution as that of the R signal; (2) the η' sideband (η'-sdb) arises from wrong combinations of $\gamma\gamma\pi^+\pi^-$ ($\gamma\pi^+\pi^-$) for the $\eta\pi\pi$ ($\gamma\rho$) mode that survive the η' selection criteria, which is estimated using the events in the margins of the η' signal in the $\eta\pi\pi$ ($\gamma\rho$) invariant-mass distribution; (3) $\eta'\pi^+\pi^- + X$ ($b_{\rm any}$) events having additional particles in the event beyond the R candidate. Other nonexclusive events, including those arising from initial-state radiation, are found to be negligible [10].

Simultaneous fits to the $\eta'\pi^+\pi^-$ mass spectra with the $\eta\pi\pi$ and $\gamma\rho$ modes combined are performed for both $\eta_c(1S)$ and $\eta_c(2S)$. The result on the fit for the $\eta_c(1S)$ signal and background contributions are shown in top two plots in Fig. 1. The $\eta_c(1S)$ mass and width are determined to be $M = [2984.6 \pm 0.7\ (\text{stat.}) \pm 2.2\ (\text{syst.})]$ MeV/c^2 and $\Gamma = [30.8^{+2.3}_{-2.2}\ (\text{stat.}) \pm 2.5\ (\text{syst.})]$ MeV, with yields of $n_1 = 945^{+38}_{-37}$ for the $\eta\pi\pi$ mode and $n_2 = 1728^{+69}_{-68}$ for the $\gamma\rho$ mode. Bottom two plots in Fig. 1 shows the result on the fit for the $\eta_c(2S)$ region, which results in a signal with a statistical significance of 5.5σ, and yields of $n_1 = 41^{+9}_{-8}$ for the $\eta\pi\pi$ mode and $n_2 = 65^{+14}_{-13}$ for the $\gamma\rho$ mode. The $\eta_c(2S)$ mass is determined to be $M = [3635.1 \pm 3.7\ (\text{stat.}) \pm 2.9\ (\text{syst.})]$ MeV/c^2; its width is fixed to the world-average value of 11.3 MeV [11] in the fit. The products of the two-photon decay width and branching fraction (B) of decays to $\eta'\pi^+\pi^-$ are determined to be $\Gamma_{\gamma\gamma}B = [65.4 \pm 2.6\ (\text{stat.}) \pm 6.9\ (\text{syst.})]$ eV for $\eta_c(1S)$ and $[5.6^{+1.2}_{-1.1}\ (\text{stat.}) \pm 1.1\ (\text{syst.})]$ eV for $\eta_c(2S)$. The first and second errors are statistical and systematic, respectively. For the systematic uncertainties in the results throughout the article, the reader is referred to paper [12].

Under the assumption of equal branching fractions for $\eta_c(1S)$ and $\eta_c(2S)$ decay, the two-photon decay width for $\eta_c(2S)$ is determined to be $\Gamma_{\gamma\gamma}(\eta_c(2S)) = (1.3 \pm 0.6)$ keV by CLEO [5], which lies at the lower bound of the QCD predictions [13]. The resulting $\Gamma_{\gamma\gamma}(\eta_c(2S))$ value, derived from this work, is less than half of CLEO's. On the other hand, the measured unequal branching fractions for $\eta_c(1S)$ and $\eta_c(2S)$ decays to $K\bar{K}\pi$, albeit with good precision for the former [11] but large uncertainty for the latter [14], indicates that an improved test of the assumption with experimental data is indeed needed.

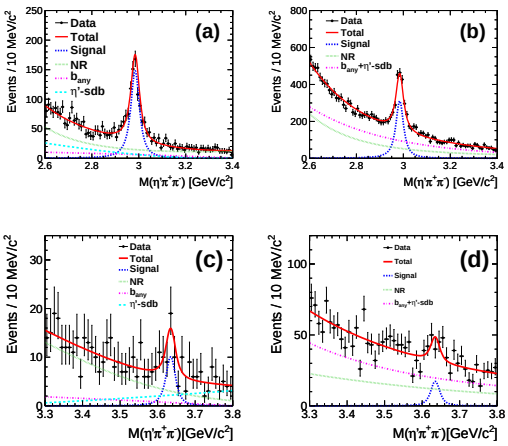

Figure 1: The invariant mass distribution for the $\eta'\pi^+\pi^-$ candidates for (a) [(c)] the $\eta\pi\pi$ mode and (b) [(d)] the $\gamma\rho$ mode, in the $\eta_c(1S)$ [$\eta_c(2S)$] region. For the definition and the curves, see [12].

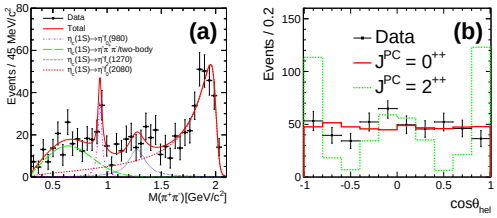

Figure 2: The fit results for the $f_0(980)$, $f_2(1270)$ and $f_0(2080)$ (a) and the distribution of cos$\theta_{\rm hel}$ for the $f_0(2080)$ candidate events (b). For the definition and the curves, see [12].

5. Study of the $\pi^+\pi^-$ invariant mass distribution

We check the $M_{\pi^+\pi^-}$ ($M_{\pi^+\pi^-,\rm sdb}$) invariant mass distribution for the events selected within the $\eta_c(1S)$ signal window $[2.90,3.06]$ GeV/c^2 (sideband region of $[2.60,2.81]\cup[3.15,3.36]$ GeV/c^2) in the $\eta\pi\pi$ mode. In addition to possible excesses at 980 MeV/c^2 and 1270 MeV/c^2 regions, an enhancement near 1960 MeV/c^2 is observed in the $\eta_c(1S)$ signal window. No such excess near 1960 MeV/c^2 is seen in the $\eta_c(1S)$ sideband region. We label it the $f_0(2080)$, with mass and spin to be given in this section. This structure, produced from $\eta_c(1S)$ decay, is observed for the first time.

The fit results for the $f_0(980)$, $f_2(1270)$ and $f_0(2080)$ components are shown in Fig. 2 (a). The $f_0(980)$ and $f_2(1270)$ yields are $n_{f_0} = 49\pm17$ and $n_{f_2} = 77^{+28}_{-29}$ with statistical significances of 3.1σ and 2.6σ, respectively. The $f_0(2080)$ yield, mass and width are determined to be $n_{f_0} = 451^{+43}_{-41}$ with a statistical significance of 20σ, $M = [2083^{+63}_{-66}(\text{stat.})\pm32(\text{syst.})]$ MeV/c^2 and $\Gamma = (178^{+60}_{-178}\pm55)$ MeV. Under the assumption of an equal rising rate of the two efficiency curves for the $\eta_c(1S)$ decays to $\eta'\pi^+\pi^-$ and $\eta' f_0(2080)$, the product of the two-photon decay width and branching fraction for the $\eta_c(1S)$ decay to $\eta' f_0(2080)$ is $\Gamma_{\gamma\gamma}B[\eta_c(1S)\to\eta' f_0(2080)] = [41.5^{+4.0}_{-3.8}(\text{stat.})\pm5.4(\text{syst.})]$ eV. The upper limit of the product for $\eta_c(1S)$ decays to $\eta' f_0(980)$ is $\Gamma_{\gamma\gamma}B[\eta_c(1S)\to\eta' f_0(980)] <$ 5.6 eV at 95% C.L.

Figure 2 (b) shows the distribution of cos$\theta_{\rm hel}$ for the $f_0(2080)$ candidate events, which are extracted by fitting the $f_0(2080)$ signal in each angular bin, together with MC expectations for $J^{PC} = 0^{++}$ and 2^{++}. Here, $\theta_{\rm hel}$ is the $f_0(2080)$ helicity angle, *i.e.,* the angle between the pion momentum and the direction of the $\gamma\gamma$ c.m. system in the $\pi^+\pi^-$ rest frame. We utilize the method previously deployed by LHCb and Belle [15] to calculate the exclusion level of the $J^{PC} = 2^{++}$ hypothesis for the $f_0(2080)$ signal. The 0^{++} hypothesis is favored over the 2^{++} hypotheses at the exclusion level of 11σ.

6. measurements of the cross sections for $\gamma \to \eta'\pi^+\pi^-$ and $\eta' f_2(1270)$ productions

We utilize the data sample selected in the $\eta' \to \eta\pi\pi$ mode to measure the non-resonant production of $\eta'\pi^+\pi^-$ final states via two-photon collisions. The differential cross section in the measurement of the W and $|\cos\theta^*|$ two-dimensional (2D) distribution for the final state particles is calculated with the formula below, accounting for the efficiencies as a function of the measured variables.

$$\frac{d\sigma_{\gamma\gamma\to h}(W,\cos\theta^*)}{d|\cos\theta^*|} = \frac{\Delta N(W,\cos\theta^*)/\varepsilon(W,\cos\theta^*)}{L_{\rm int}\frac{dL_{\gamma\gamma}(W)}{dW}\Delta W\Delta|\cos\theta^*|}, \tag{6.1}$$

where the yield ΔN is extracted by fitting the $|\Sigma p_t^*|$ $[M(\pi^+\pi^-)]$ distribution in a data subsample sliced in each 2D bin for the $\gamma\gamma \to \eta'\pi^+\pi^-$ $[\gamma\gamma \to \eta' f_2(1270)]$ production. The efficiency $\varepsilon(W,\cos\theta^*)$ is evaluated using MC events for each 2D bin. $L_{\rm int}$ is the total integrated luminosity of the data.

In the left plot of Fig. 3, the measured W-dependent cross sections of $\gamma\gamma \to \eta' f_2(1270)$ and $\gamma\gamma \to \eta'\pi^+\pi^-$ [including $\eta' f_2(1270)$] production are shown. Taking the difference between the two yields in each 2D bin in data as input, the cross sections of $\gamma\gamma \to \eta'\pi^+\pi^-$ production without the $\eta' f_2(1270)$ contribution for the $\eta\pi\pi$ mode are calculated and shown in the right plot of Fig. 3. Two peaking structures are evident. The one around 1.8 GeV likely arises from the $\eta(1760)$ and $X(1835)$ decays to $\eta'\pi^+\pi^-$ [10] and the other around 2.15 GeV is possibly due to $\gamma\gamma \to X(2100) \to \eta' f_0(980)$ production. The $\eta_c(1S)$ contribution near 2.98 GeV has been subtracted. A larger data sample is necessary in order to understand these two structures in more detail.

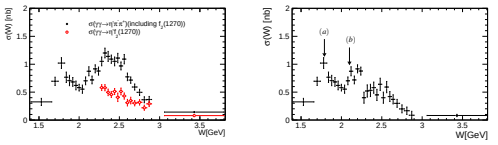

Fig 3: Left panel: cross sections of $\gamma\gamma \to \eta'\pi^+\pi^-$ [including $\eta' f_2(1270)$] (black solid dots) and $\gamma\gamma \to \eta' f_2(1270)$ (red open dots). Right panel: cross sections of $\gamma\gamma \to \eta'\pi^+\pi^-$ [excluding $\gamma\gamma \to \eta' f_2(1270)$] in the W range above 2.26 GeV.

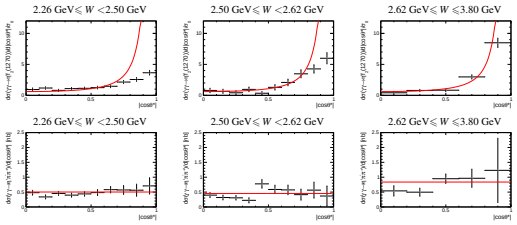

Figure 4: Top (Bottom) three plots are the Cross sections of $\gamma\gamma \to \eta' f_2(1270)$ [$\gamma\gamma \to \eta'\pi^+\pi^-$ [excluding $\eta' f_2(1270)$] in $|\cos\theta^*|$] in three W regions.

Top three plots in Fig. 4 show the differential cross sections in $|\cos\theta^*|$ for $\gamma\gamma \to \eta' f_2(1270)$. All the plots show an ascending trend, and its rate of increase is greater for events in the larger W ranges. The complicated behavior for the angular dependence of the cross sections is seen in the range of $W < 2.50$ GeV with markedly lower power for $\sin\theta^*$ of $\alpha < 4$, while it tends to match with the power law for the ranges of $W \in [2.50, 2.62]$ and $[2.62, 3.80]$ GeV.

The differential cross section in $|\cos\theta^*|$ for $\gamma\gamma \to \eta'\pi^+\pi^-$ production after subtracting both contributions from $\gamma\gamma \to \eta' f_2(1270)$ in the W region above 2.26 GeV and $\eta_c(1S)$ in the region of

$W \in [2.62, 3.06]$ GeV is shown in bottom three plots of Fig. 4. Nearly flat distributions of the cross sections in the three regions of $W \in [2.26, 2.50]$, $[2.50, 2.62]$ and $[2.62, 3.06]$ GeV are consistent with the expectations from three-body final-state production via two-photon collisions.

7. summary

In summary, the $\eta_c(1S)$, $\eta_c(2S)$ and non-resonant $\eta'\pi^+\pi^-$ production via two-photon collisions is measured. We report the first observations of the signals for $\eta_c(1S)$ decays to $\eta' f_0(2080)$ with $f_0(2080) \to \pi^+\pi^-$ and $\eta_c(2S)$ decays to $\eta'\pi^+\pi^-$, the measured products of the two-photon decay width and the branching fraction for the $\eta_c(1S)$ and $\eta_c(2S)$ decays to $\eta'\pi^+\pi^-$, and the measurement of non-resonant production of two-body $\eta' f_2(1270)$ and three-body $\eta'\pi^+\pi^-$ final states via two-photon collisions.

References

[1] N. Brambilla *et al.*, Eur. Phys. C **71**, 1534 (2011).

[2] J. P. Lansberg and T. N. Pham, Phys. Rev. D **74**, 034001 (2006).

[3] N. Brambilla, A. Pineda, J. Soto, A. Vairo, Rev. Mod. Phys. **77**, 1423 (2005).

[4] M. Ablikim *et al.* (BESIII Collaboration), Phys. Rev. Lett. **108**, 222002 (2012); M. Ablikim *et al.* (BESIII Collaboration), Phys. Rev. D **86**, 092009 (2012); M. Ablikim *et al.* (BESIII Collaboration), Phys. Rev. Lett. **109**, 042003 (2012); P. del Amo Sanchez *et al.* (BaBar Collaboration), Phys. Rev. D **84**, 012004 (2011); A. Vinokurova *et al.* (Belle Collaboration), Phys. Lett. B **706**, 139 (2011); S. Uehara *et al.* (Belle Collaboration), Eur. Phys. J. C **53**, 1 (2008).

[5] D.M. Asner *et al.* (CLEO Collaboration), Phys. Rev. Lett. **92**, 142001 (2004). The value 1.3 ± 0.6 keV by CLEO is calculated using $\Gamma_{\gamma\gamma}(\eta_c(1S))$ = $(7.4 \pm 0.4 \pm 2.3)$ keV of the CLEO's as input.

[6] S. J. Brodsky and G. P. Lepage, Phys. Rev. D **24**, 1808 (1981); V. L. Chernyak and A. R. Zhitnitsky, Phys. Rept. **112**, 173 (1984); M. Benayoun and V. L. Chernyak, Nucl. Phys. **B329**, 285 (1990).

[7] M. Diehl, P. Kroll and C. Vogt, Phys. Lett. B **532**, 99(2002).

[8] A.J. Bevan, B. Golob, Th. Mannel, S. Prell and B.D. Yabsley, Eds., Eur. Phys. Jour. C **74**, 3026 (2014); see Section 22.2.2.

[9] A. Abashian *et al.* (Belle Collaboration), Nucl. Instrum. Methods Phys. Res. Sect. A **479**, 117 (2002); also see detector section in J.Brodzicka *et al.*, Prog. Theor. Exp. Phys. **2012**, 04D001 (2012).

[10] C.C. Zhang *et al.* (Belle Collaboration), Phys. Rev. D **86**, 052002 (2012).

[11] C. Patrignani *et al.* (Particle Data Group), Chin. Phys. C **40**, 100001 (2016).

[12] Q. N. Xu et al. (Belle Collaboration), arXiv:1805.03044[hep-ex] (2018).

[13] E. S. Ackleh and T. Barnes, Phys. Rev. D **45**, 232 (1992); M. R. Ahmady and R. R. Mendel, Phys. Rev. D **51**, 141 (1995); C. R. Munz, Nucl. Phys. A **609**, 364 (1996); H.W. Huang, J. H. Liu, J. Tang and K. T. Chao, Phys. Rev. D **56**, 368 (1997); D. Ebert, R. N. Faustov and V. O. Galkin, Mod. Phys. Lett. A **18**, 601 (2003); C. S. Kim, T. Lee and G. L. Wang, Phys. Lett. B **606**, 323 (2005).

[14] B. Aubert *et al.* (BaBar Collaboration), Phys. Rev. D **78**, 012006 (2008).

[15] R. Aaij *et al.* (LHCb Collaboration), Phys. Rev. Lett. **110**, 222001 (2013); K. Chilikin *et al.* (Belle Collaboration), Phys. Rev. D **88**, 074026 (2013).